Egypt.J.Chem. **Vol. 63**, No.10 . pp. 3641- 3654 (2020)

Egyptian Journal of Chemistry
http://ejchem.journals.ekb.eg/

Kinetics and Thermodynamics of Aqueous Copper Adsorption by Ca-Al-Zn LDH and Its Calcined Product

Al-Sayed A. Bakr[1*], Reda R. Abdel Gayed[2], Radwan M. El-Zoheiry[3], Ahmed A. Salem[1]

[1] *Egyptian Petroleum Research Institute (EPRI), Nasr City, Cairo 11727, Egypt.*
[2] *Giza North Power Station, Ministry of Electricity And Energy, Giza, Egypt.*
[3] *Department of Mechanical Power Engineering, Faculty of Engineering, Benha University, Benha, Qalubia, Egypt.*

THE Ca-Al-Zn layered double hydroxide (LDH) which synthesized by the co-precipitation method and its calcined product was used in the removal of Cu(II) from aqueous solutions. At optimum conditions, the calcined Ca-Al-Zn LDH product has a higher potential application in the cupreous ion's adsorption field (45.2mg/g) than the uncalcined LDH (38.8mg/g). Langmuir and Freundlich models were used to optimizing the adsorption process and pseudo-first and pseudo-second-order models were used to evaluating the adsorption kinetics of Cu(II) onto Ca-Al-Zn LDH and its calcined product. Langmuir model fitted the experimental data better than Freundlich model and the pseudo-first-order model is more sufficient to depict the adsorption kinetics. From thermodynamic studies; Gibbs free energy (ΔG°), Enthalpy change (ΔH°), and Entropy change (ΔS°) revealed that the adsorption processes are spontaneous, endothermic, and randomness processes at the solid-solution interface during adsorption.

Keywords: Water treatment, Kinetics, Thermodynamics, Ca-Al-Zn LDH, Cu(II) adsorption.

Introduction

Large amounts of metal-contaminated wastewater from industries and other sources consist of many heavy metals such as Fe, Cd, Cr, Cu, Ni, Mn, As, Hg, Pb, and Zn which are the most pollutants present in the chemical-intensive industries and human waste. Heavy metals have a high solubility in aquatic environments, they can be absorbed by living organisms and large concentrations of them may accumulate in the human body. When the heavy metals are taken out of allowed concentration, they can cause serious health disorders [1-6]. Accordingly, it is necessary to remove these pollutants like heavy metals from wastewater prior to polluting the environment. These heavy metals removed from the inorganic stream by traditional treatment processes such as chemical precipitation, ion exchange, and electrochemical removal processes. These operations have a lot of troubles such as high-energy needing, incomplete removal, and producing a toxic sludge [7]. Latterly, some developments regarding the more, higher, and cheaper effective treatment processes such as adsorption technology which has become one of the possible treatment techniques [8]. There are different types of these adsorbents such as biological or organic origin, mineral, a byproduct of industry, wastes of agriculture, and natural or synthetic materials [9].

The adsorption of biosynthesized melanin for copper ions (Cu(II)) was well illustrated by the pseudo-second-order model and the equilibrium data well fitted to Langmuir isotherm with a maximum adsorption capacity of 167.8 mg/g. The thermodynamic parameters revealed that the adsorption of Cu(II) on melanin was favorable, spontaneous, and endothermic in nature [10]. The adsorption of Cu(II) on $CaTiO_3$ powders was well illustrated by the pseudo-second-

*Corresponding author: als_water@yahoo.com
Received 30/3/2020; Accepted 4/6/2020
DOI: 10.21608/ejchem.2020.26924.2553

order adsorption kinetics and it will be fitted by Langmuir adsorption isotherm. The adsorption process was spontaneous and endothermic and the maximum adsorption capacity was 66.4 mg g^{-1} [11]. The adsorption of Cu(II) on titanate nanocomposite was well fitted by the pseudo-second-order adsorption kinetic and Langmuir adsorption models and the maximum adsorption capacity was 13.8 mg g^{-1}. The thermodynamic parameters revealed that the adsorption of these ions was spontaneous and endothermic [12]. The adsorption equilibrium by copper (Cu^{2+}) onto multi-walled carbon nanotubes (MWCNT) was described well by the Langmuir isotherm model and pseudo-second-order adsorption kinetic with a maximum adsorption capacity of 12.34 mg/g. The thermodynamics parameters pointed at spontaneous and endothermic nature of the adsorption process [13]. The elimination of copper ions from aqueous solutions by poly(N-vinylpyrrolidone) reached 3.27 $mg.g^{-1}$. Equilibrium data were well fitted with the Langmuir and the experimental data follow well the pseudo-second-order kinetics. The thermodynamic parameters show spontaneous and exothermic adsorption process with a negative value of ΔS° [14]. The adsorption of Cu(II) ions by *Albizia lebbeck* pods as agricultural waste was fitted well with the Langmuir isotherm model with correlation coefficient (R^2> 0.94), whereas the adsorption kinetics followed the pseudo-second-order kinetics. The thermodynamic parameters proved that adsorption process is endothermic and non-spontaneous at low temperatures, while spontaneity occurred at higher temperatures [15].

This study is a continuation of our study in determining the potential of Ca-Al-Zn LDH and its calcined product as adsorbents for Cu(II) ions from aqueous solutions. The paper deals with Langmuir and Freundlich models to optimizing the adsorption process and the pseudo-first-order and pseudo-second-order models were used to evaluating the adsorption kinetics of Cu(II) onto Ca-Al-Zn LDH and its calcined product. Also, thermodynamic parameters (ΔG°, ΔH° and ΔS°) are studied.

Materials and experimental

Materials

The used materials have high analytical purity. Copper nitrate pentahemihydrate [$(Cu(NO_3)_2 \cdot 2½H_2O)$], aluminum nitrate nonahydrate [$Al(NO_3)_3.9H_2O$], potassium carbonate [K_2CO_3], and potassium hydroxide [KOH] were purchased from Sigma-Aldrich Co. Calcium nitrate tetrahydrate [$Ca(NO_3)_2 \cdot 4H_2O$]; and zinc nitrate hexahydrate [$Zn(NO_3)_2 \cdot 6H_2O$] were purchased from Loba Chemie Co [16].

Synthesis of Ca-Al-Zn LDH

The Co-precipitation is the method used in the preparation of Ca-Al-Zn LDH. Firstly, a salt solutions containing $Al(NO_3)_3.9H_2O$, $Ca(NO_3)_2.4H_2O$ and $Zn(NO_3)_2.6H_2O$ were prepared in the required amounts in an equimolar ratio to prepare a solution A. Alkaline solution (2M) containing K_2CO_3 and KOH was prepared at a controlled pH of 9 (solution B). Then, the solutions A and B are mixed in a glass reactor containing deionized water; the formed precipitate is stirred for 18 hours at 80°C. After that, the formed precipitate was washed with deionized water and then dried at 100°C for 24 h. The obtained Ca-Al-Zn LDH was calcined for 5h at 450°C prior to adsorption. The structure, composition, and morphology of synthesized materials were deeply discussed in our previous study [16].

Metal adsorption

Adsorption of copper ions onto calcined and uncalcined of Ca-Al-Zn LDH was studied at constant pH 6, the adsorbent dosage of 0.25g/l and stirring rate of 160 rpm, and at different initial metal concentrations (45, 55, 65, 75, 85, 95, 105, 115, 125 and 135mg/l), different contact times (10, 20, 30, 60, 90, 120, 150 and 180 minutes) and different temperatures (298, 313 and 328K). The pH value of solutions was adjusted using a standard acid solution (0.01M HNO_3) and standard alkaline solution (0.125M NaOH). Buffer solutions of pH 4.0, 7.0 and 10.0 were used to adjusting the solution pH and measured by pH meter (Thermo Orion 5 Star). At different times of reactions, the samples of solutions were taken and the metal concentrations were determined using Spectrophotometer, LaMotte, model SMART spectro, USA.

The adsorption capacity and the removal percentage were determined using the following two equations [17,18]:

$$q_e = \frac{(C_0 - C_e)v}{m} \quad (1)$$

$$\text{Removal } \% = \frac{(C_0 - C_e)}{C_0} \times 100\% \quad (2)$$

where, q_e represents the adsorption capacity at equilibrium (mg of adsorbate/g of adsorbent),

V represents the volume of solute solution (l), C_0 represents the initial concentration of solute (mg/l), C_e represents the residual concentration of solute after adsorption (mg/l) and m represents the weight of adsorbent (g).

Kinetic studies

Pseudo-first order model

The kinetic process of liquid-solid phase adsorption was described by equation of the pseudo-first-order model which is the earliest model pertaining to the adsorption rate based on the adsorption capacity [19, 20].

The linear form of the pseudo-first order model equation is:

$$\log(q_e - q_t) = \log q_e - \left(\frac{k_1 t}{2.303}\right) \quad (3)$$

where, q_t and q_e are the amounts of adsorbate adsorbed at a definite time and at equilibrium, respectively. k_1 is the constant of pseudo-first-order rate which can be calculated from the plot of log (q_e - q_t) vs. t.

Pseudo-second order model

The chemisorption reaction involving valence forces through exchange or sharing of electrons between adsorbent and adsorbate was indicated by equation of the pseudo-second order model [20].

The linear form of pseudo-second-order model equation is:

$$\frac{t}{q_t} = \frac{1}{k_2 (q_e)^2} + \left(\frac{1}{q_e}\right) t \quad (4)$$

where k_2 is the constant of pseudo-second-order rate which can be calculated from the slope and intercept of t/q_t vs. t plot.

Adsorption studies

As a function of concentration at a constant temperature, the amount of adsorbed material is determined and the function resulted here is called adsorption isotherm. There are many isotherm models e.g. linear isotherm, Temkin, BET, Langmuir and Freundlich, but the most commonly used models are Langmuir and Freundlich. These models are used in water treatment especially for monolayer and noncompetitive adsorption processes which described by development of experimental isotherm data [21,22].

The accordance of predicted and experimental values calculated by isotherm models is expressed by the correlation coefficient (R^2). The more applicable model is the nearest to one of the relatively high values of the correlation coefficient.

Langmuir's adsorption

The monolayer adsorption onto a surface containing a certain number of many sites supposes regular energies and transmigration on that adsorbate surface and it conforming to the isotherm of Langmuir's adsorption. The maximum adsorption capacity of adsorbent formed from a complete monolayer covering the surface is determined by Langmuir isotherm model [22].

The linear form of Langmuir's isotherm equation is:

$$\frac{C_e}{q_e} = \frac{1}{k_L b} + \frac{C_e}{b} \quad (5)$$

where C_e is the amount of adsorbate at equilibrium time (mg), b and k_L are the maximum adsorption capacity (mg/g), and the Langmuir constants (l/mg) (related to adsorption energy), respectively. These constants can be calculated from the plot of C_e/q_e vs. C_e, while b is 1/intercept, and k_L is equal to the intercept x 1/slope.

Freundlich adsorption

The heterogeneous surface energies were determined by Freundlich adsorption isotherm and the ratio of quantity of solute adsorbed on a known mass of adsorbent to different concentrations of solute was presented by this isotherm. The Langmuir's energy varies with adsorption capacity (q_e) due to variation of the adsorption heat [18].

The linear form of Freundlich isotherm equation is:

$$\log q_e = \log K_f + \left(\frac{1}{n}\right) \log C_e \quad (6)$$

where K_f (l/mg) is the constant of Freundlich isotherm (related to the sorption capacity) and n is the heterogeneity factor (related to the sorption intensity). These constants can be calculated from the plot of Log q_e vs. Log C_e.

The adsorption rate is remarkable to reaching the equilibrium state and it happens through three proceedings; firstly, when the adsorbate is diffuse through a surface layer to the outer surface of adsorbent, secondly the adsorbate is diffuse inside the pores of adsorbent and finally, the adsorption takes place between the adsorbate and adsorbent [23].

Thermodynamic calculations

The spontaneity of the adsorption process can be determined by energy and entropy considerations

and the values of the thermodynamic parameters are perfect indicators for practical application of the adsorption process.

At equilibrium of adsorption process, the change in Gibbs free energy (ΔG°) can be written as follows [24,25]:

$$\Delta G^{o} = -RT \ln b \quad (7)$$

where T is the temperature (K), R is gas constant (8.314 $kJmol^{-1}K^{-1}$) and b is Langmuir equilibrium constant. Therefore, for an adsorption reaction can be estimated at different temperatures if Langmuir equilibrium constant, for the adsorption mechanism is known.

The rest constants of thermodynamic parameters of adsorption process can be resulted from b values at different temperatures by equation of Van't Hoff [61]:

$$\ln b = \frac{\Delta S^{o}}{R} - \frac{\Delta H^{o}}{RT} \quad (8)$$

where ΔS° and ΔH° are entropy and enthalpy changes respectively, and a straight line with slope (ΔH°/R) and intercept (ΔS°/R) can be obtained from plotting lnb versus 1/T.

Results and Discussion

Characterization of Ca-Al-Zn LDH and its calcined product

The characterization of the prepared Ca-Al-Zn LDH and its calcined product were discussed in our previous study [16].

Influence of adsorption contact time

The adsorption contact times (10-180 minutes) required for the maximum adsorption capacities of copper ions by Ca-Al-Zn LDH and its calcined product at different temperatures, initial concentration of 115mg/l, adsorbent dosage of 0.25g/l, pH 6.0 and stirring rate of 160rpm are shown in Figure 1. There is an increment in adsorption capacity appeared for all temperatures in the case of Ca-Al-Zn LDH and its calcined product for adsorption process. In the initial stages of Cu(II) adsorption, the adsorption capacity fastly increased with increasing contact time (optimum time is 120min) and increasing temperature (optimum temperature is 328K), to be 38.8mg/g for Ca-Al-Zn LDH and 45.2mg/g for calcined Ca-Al-Zn LDH. This is attributed to the availability of large surface areas and more pores of adsorbents in the initial period. After 180min, a little increment happens reached to 40.7mg/g in the case of Ca-Al-Zn LDH and 46.0mg/g in the case of calcined Ca-Al-Zn LDH. The slow rate of adsorption at this stage may be due to the agglomeration of copper ions on all pores of adsorbent surface [26,27].

Kinetics evaluation

The pseudo-first and pseudo-second-order models {equations (3,4)} were applied to evaluate the adsorption kinetics of Cu(II) ions onto Ca-Al-Zn LDH and its calcined product. Linear plots of $\log(q_e-q_t)$ versus t (pseudo-first-order model) and t/q_t versus t (pseudo- second-order model) are depicted in Figures 2 and 3 for Ca-Al-Zn LDH and its calcined product at 298, 313 and 328K, respectively.

The data obtained from those figures are listed in Table 1. These data revealed that the correlation coefficients for the pseudo-first and pseudo-second orders are suitable to describe the Cu(II) adsorption process at different temperatures. The correlation coefficients for the pseudo-first-order (R^2 = 0.987 and 0.963) and (R^2 = 0.974 and 0.972) were higher than for the pseudo-second-order (R^2 = 0.758 and 0.924) and (R^2 = 0.787 and 0.953) at 298 and 313K for uncalcined and calcined LDHs, respectively. While, the data revealed that by increasing temperature to 328K, the correlation coefficients for the pseudo-second-order (R^2 = 0.933 and 0.986) were higher than that for pseudo-first-order (R^2 = 0.922 and 0.932) for uncalcined and calcined LDHs, respectively. This referred that the system is more appropriately described by the pseudo-first order model at low temperature, while at a higher temperature; the system is more appropriately described by the pseudo-second-order model.

At low temperature, the pseudo-first-order model assuming the adsorption process depending only on metal ions numbers present in aqueous solution and the availability of binding sites on the adsorbent surface at a definite particular period. While at the higher temperature, the pseudo-second-order model assuming the adsorption process is chemical adsorption [28-30].

Influence of initial Cu(II) concentration

The adsorption capacities resulted in different initial Cu(II) concentrations (45-135 mg/l) for uncalcined and calcined Ca-Al-Zn LDHs are shown in Figure 4. The increase in adsorption capacity was observed with increasing initial copper ion concentrations from 45 to 95mg/l at all temperatures (298,313 and 328K). The adsorption capacities from initial copper ion

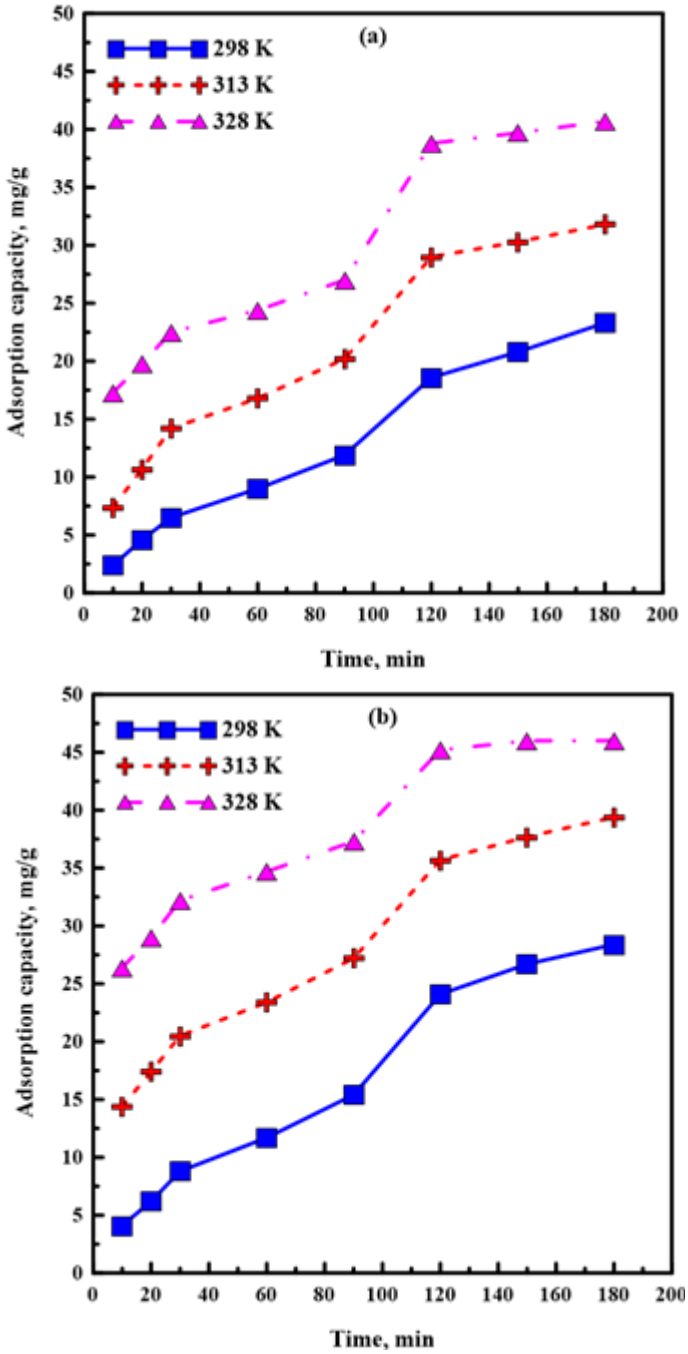

Fig. 1. Effect of contact time on the adsorption capacity of Cu(II) onto (a) uncalcined Ca-Al-Zn LDH and (b) calcined Ca-Al-Zn LDH at different temperatures, initial concentration of 115mg/l, adsorbent dosage of 0.25g/l, pH 6.0 and stirring rate of 160rpm.

concentrations of 95mg/l were 37.2 and 38.0mg/g for uncalcined and calcined Ca-Al-Zn LDHs at higher temperature (328K), respectively. A little increment happened in adsorption capacities for 115mg/l of initial copper concentration reached to 38.8mg/g in the case of Ca-Al-Zn LDH and 45.2mg/g in case of its calcined LDH. This increment in uptake capacity was due to the higher concentration gradient, which is a driving force to overcome the mass transfer resistance between the liquid/solid phases. While at higher concentrations (>115 mg/l), the saturation of adsorption binding sites may have occurred. This behavior is attributed to less availability of

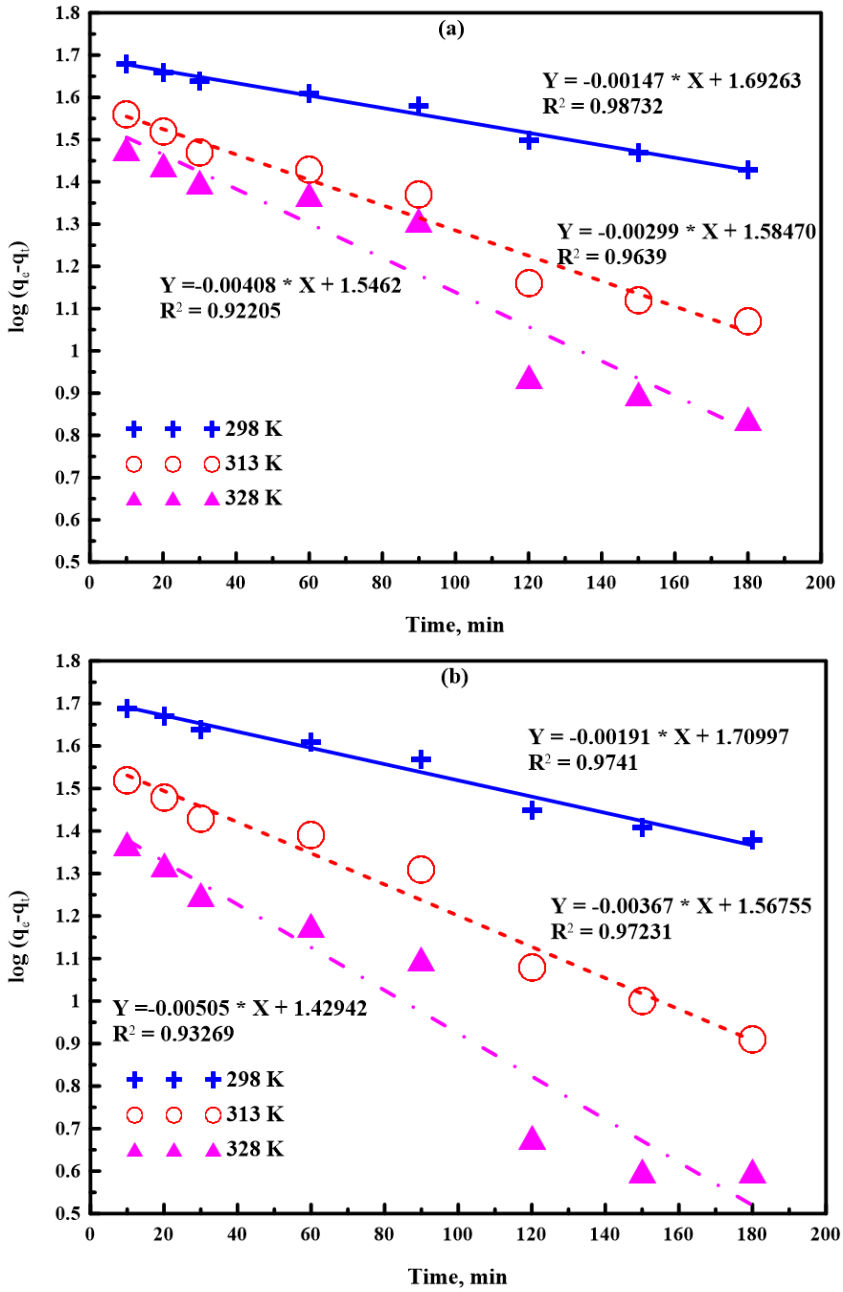

Fig. 2. Adsorption kinetics of pseudo-first-order models for adsorption of Cu(II) on (a) uncalcined Ca-Al-Zn LDH and (b) calcined Ca-Al-Zn LDH at different temperatures, initial concentration of 115mg/l, adsorbent dosage of 0.25g/l, pH 6.0 and stirring rate of 160rpm.

surface-active sites [31-33].

Adsorption isotherms evaluation

Adsorption isotherms are evaluated by Langmuir and Freundlich models. The suitability of a certain adsorption isotherm to describe the obtained data depends on the correlation coefficients (R^2) of the profile [34]. According to Figures 5 and 6, Freundlich (K_F and n) and Langmuir (k_L and b) constants were evaluated from the intercept and slope of the linear plot of log q_e versus log C_e (for Freundlich model) and the linear plot of C_e/q_e versus C_e (for Langmuir model) and they are given in Table 2, which summarizes the correlation coefficients and Langmuir and Freundlich constants. The results showed that the correlation coefficients for Langmuir model were 0.996, 0.999 and 0.999 and for Freundlich model was 0.930, 0.958 and 0.920 for uncalcined

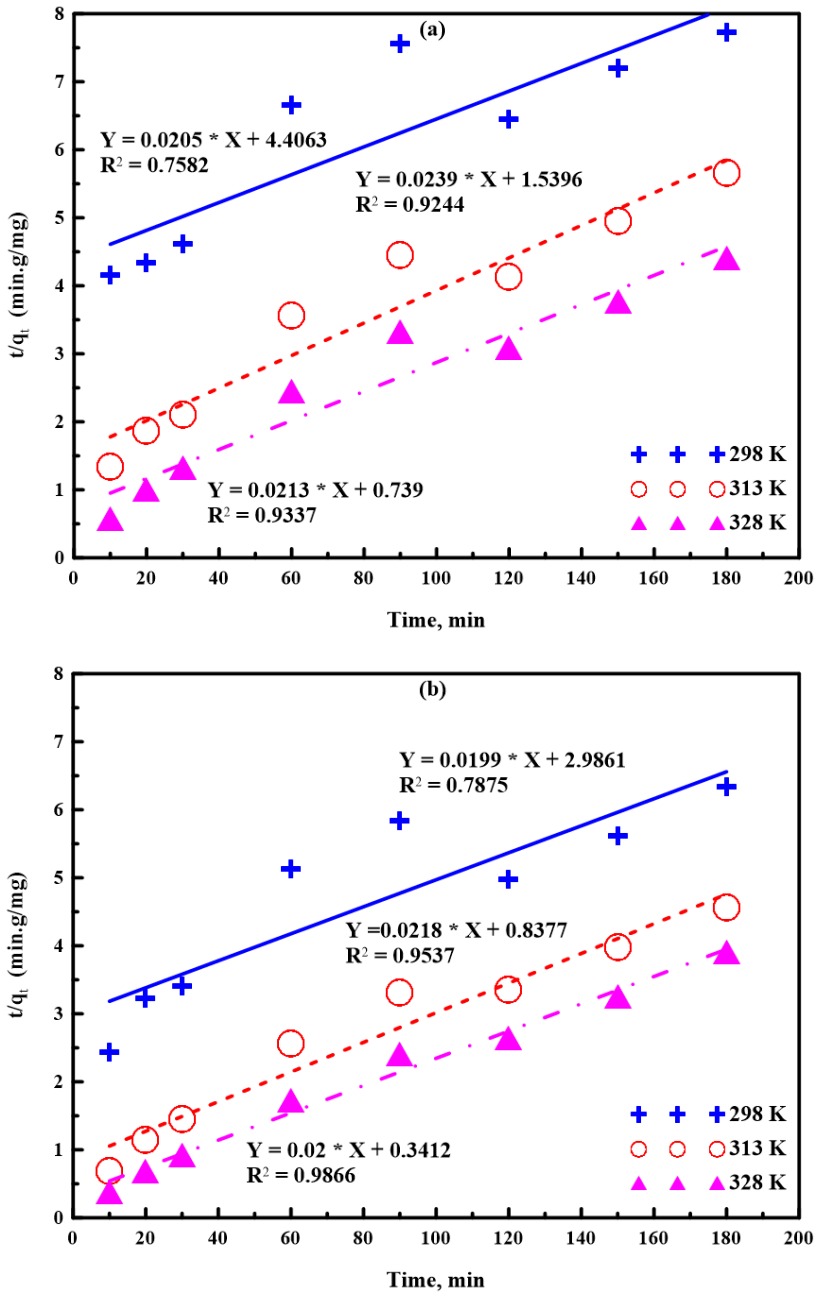

Fig. 3. Adsorption kinetics of pseudo-second-order models for adsorption of Cu(II) on (a) uncalcined Ca-Al-Zn LDH and (b) calcined Ca-Al-Zn LDH at different temperatures, initial concentration of 115mg/l, adsorbent dosage of 0.25g/l, pH 6.0 and stirring rate of 160rpm.

Ca-A-l-Zn LDH at different temperatures 298, 308 and 318K, respectively. While the correlation coefficients for Langmuir model recorded 0.999, 0.999, and 1.0 at temperatures 298, 308, and 328K for calcined Ca-A-l-Zn LDH and Freundlich model recorded 0.989, 0.980 and 0.940 at the same temperatures, respectively.

Where the correlation coefficients for Langmuir model were higher than for Freundlich model, the Cu^{2+} adsorption process is more appropriately described by Langmuir model than Freundlich one. This indicates the homogeneity of active sites on the LDHs surfaces and it means that the whole surface has identical adsorption activity and the adsorbed copper ions don't interact or compete with each other and the chemisorption reaction is the principal mechanism in adsorption process. Also, the observed increment in k_L and b

TABLE 1. Kinetic parameters of pseudo-first- and pseudo-second-order models for Cu(II) adsorption on Ca-Al-Zn LDH and its calcined LDH product at different temperatures, initial concentration of 115mg/l, adsorbent dosage of 0.25g/l, pH 6.0 and stirring rate of 160rpm.

Sample	T (k)	Pseudo first-order kinetic model			Pseudo second-order kinetic model		
		k_1 (min^{-1})	q_e (mg/g)	R^2	k_2 ($gmg^{-1}Lmin^{-1}$)	q_e (mg/g)	R^2
Uncalcined Ca-Al-Zn LDH	298	2.3×10^{-3}	49.2	0.987	9.1×10^{-5}	50.0	0.758
	313	6.9×10^{-3}	38.4	0.963	3.4×10^{-4}	43.5	0.924
	328	9.2×10^{-3}	35.2	0.922	6.0×10^{-4}	47.6	0.933
Calcined Ca-Al-Zn LDH	298	2.3×10^{-3}	51.3	0.974	1.2×10^{-4}	52.6	0.787
	313	6.9×10^{-3}	36.9	0.972	5.3×10^{-4}	47.6	0.953
	328	0.011	26.9	0.932	1.2×10^{-3}	50.0	0.986

TABLE 2. Isotherm parameters for Cu(II) adsorption onto Ca-Al-Zn LDH and its calcined LDH product at different temperatures, adsorbent dosage of 0.25g/l, pH 6.0, stirring rate of 160rpm and contact time of 120min.

Sample	T (k)	Langmuir isotherm model			Freundlich isotherm model		
		k_L (L/mg)	b (mg/g)	R^2	K_F (mg/g)	n	R^2
Uncalcined Ca-Al-Zn LDH	298	0.08	21.83	0.996	36.74	59.17	0.930
	313	0.31	31.06	0.999	19.44	9.51	0.958
	328	1.4	39.84	0.999	8.83	5.8	0.920
Calcined Ca-Al-Zn LDH	298	0.177	26.67	0.999	15.10	8.68	0.989
	313	1.92	36.76	0.999	30.37	20.92	0.980
	328	5.88	46.08	1	45.03	52.63	0.940

(in case of Langmuir model) and k_F and n (in case of Freundlich model) with increasing temperature may be due to the increment in the stability of binding forces between Cu^{2+} ions and LDH surface [35,36].

Adsorption thermodynamics

Thermodynamics parameters of copper ions removal by Ca-Al-Zn LDH and its calcined product were determined at various temperatures (298, 313, and 328K). The Gibbs free energy (ΔG°) was calculated by equation 7, while Enthalpy change (ΔH°) and Entropy change (ΔS°) were calculated according to equation 8. Thermodynamic constants are determined from the plot of lnb against 1/T in Figure 7 and showed in Table 3. The results of thermodynamic calculations showed that the values of ΔG° decreased with increasing the temperature, -7.62, -8.94 and -10.02kJmol^{-1} for Ca-Al-Zn LDH and -8.11, -9.35 and -10.43kJmol^{-1} for calcined LDH product, respectively, indicating spontaneous cupreous ions by adsorbents and the adsorption become more favorable at higher temperature due to the presence of a more driving force of Cu(II) adsorption [37]. The positive values of ΔH° (16.12 and 14.76KJ mol^{-1} for Ca-Al-Zn LDH and its calcined product, respectively) indicate that there is an endothermic behavior of the adsorption reaction and they suggest that there is

TABLE 3. Thermodynamic constants for adsorption of Cu(II) onto Ca-Al-Zn LDH and its calcined LDH product at various temperatures, adsorbent dosage of 0.25g/l, pH 6.0, stirring rate of 160rpm and contact time of 120min.

Sample	T (k)	ln b	ΔG^o (kJ mol^{-1})	ΔH^o (kJ mol^{-1})	ΔS^o (J $mol^{-1}K^{-1}$)	R^2
Uncalcined Ca-Al-Zn LDH	298	3.08	- 7.62	16.12	79.8	0.996
	313	3.44	- 8.94			
	328	3.68	- 10.02			
Calcined Ca-Al-Zn LDH	298	3.28	- 8.11	14.76	76.9	0.998
	313	3.60	- 9.35			
	328	3.83	- 10.43			

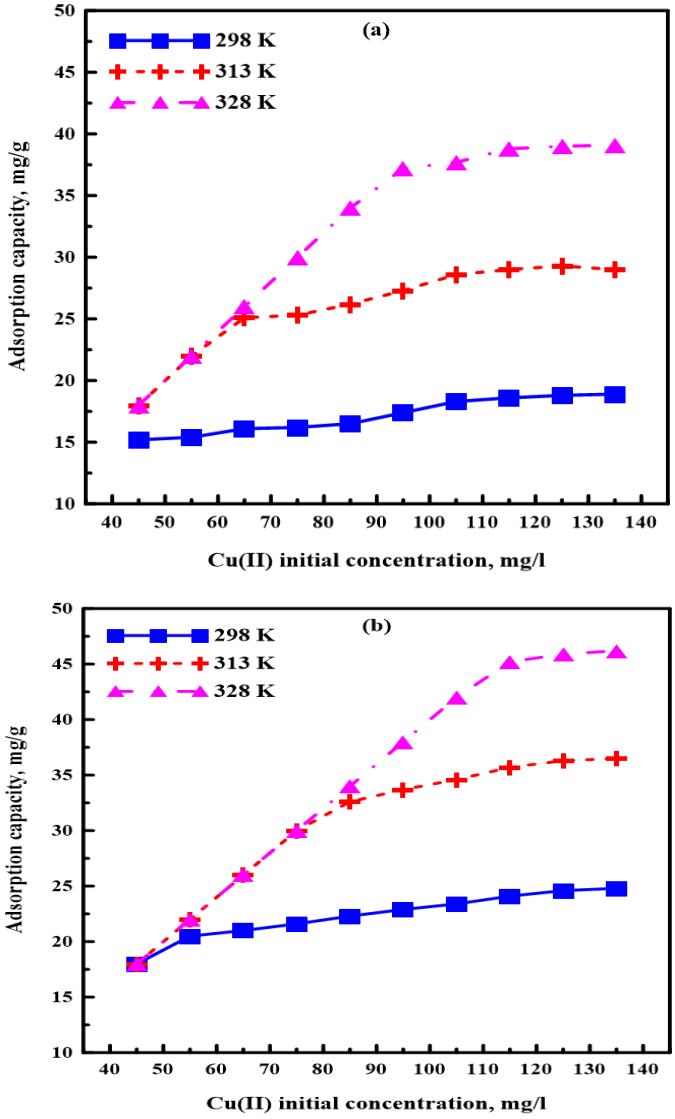

Fig. 4. Effect of Cu(II) initial concentration on adsorption capacity of (a) uncalcined Ca-Al-Zn LDH and (b) calcined Ca-Al-Zn LDH at different temperatures, adsorbent dosage 0.25g/l, pH 6.0, stirring 160rpm and contact time 120min.

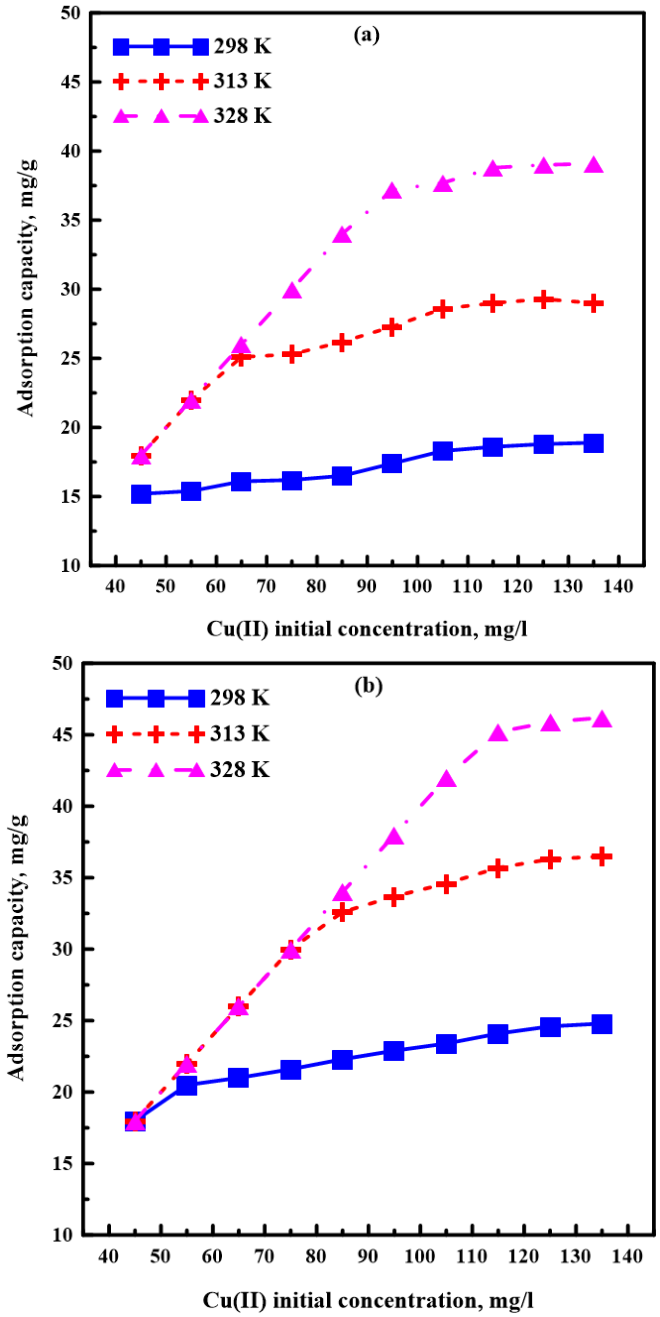

Fig. 4. Effect of Cu(II) initial concentration on adsorption capacity of (a) uncalcined Ca-Al-Zn LDH and (b) calcined Ca-Al-Zn LDH at different temperatures, adsorbent dosage 0.25g/l, pH 6.0, stirring 160rpm and contact time 120min.

a large amount of heat was consumed to transfer the copper ions from aqueous solution to solid phase [35,38].

The positive ΔS° values (79.8 and 76.9KJ mol^{-1} for Ca-Al-Zn LDH and its calcined product, respectively) revealed that there is an increase in randomness at the interface of solid-solution during the Cu(II) adsorption process [34].

Conclusions

The synthesized Ca–Al–Zn LDH and its calcined LDH product were examined in Cu(II) adsorption from aqueous solutions. The optimum conditions required for producing maximum adsorption capacities of copper ions by Ca-Al-Zn LDH(38.8mg/g) and its calcined product (45.2mg/g) were 328K of temperature, 120 min

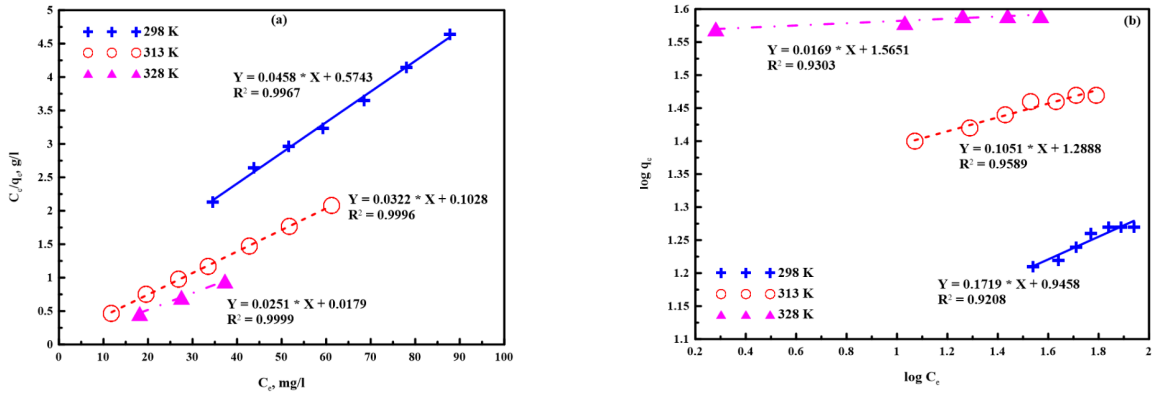

Fig. 5. Adsorption isotherm models: (a) Langmuir and (b) Freundlich for Cu(II) removal by uncalcined Ca-Al-Zn LDH at different temperatures, adsorbent dosage of 0.25g/l, pH 6.0, stirring rate of 160rpm and contact time of 120min.

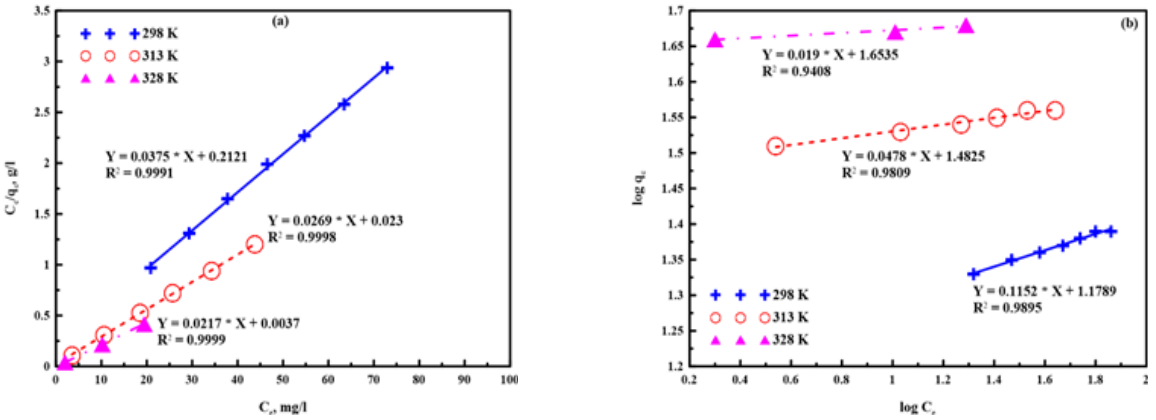

Fig. 6. Adsorption isotherm models: (a) Langmuir and (b) Freundlich for Cu(II) removal by calcined Ca-Al-Zn LDH at different temperatures, adsorbent dosage of 0.25g/l, pH 6.0, stirring rate of 160rpm and contact time of 120min.

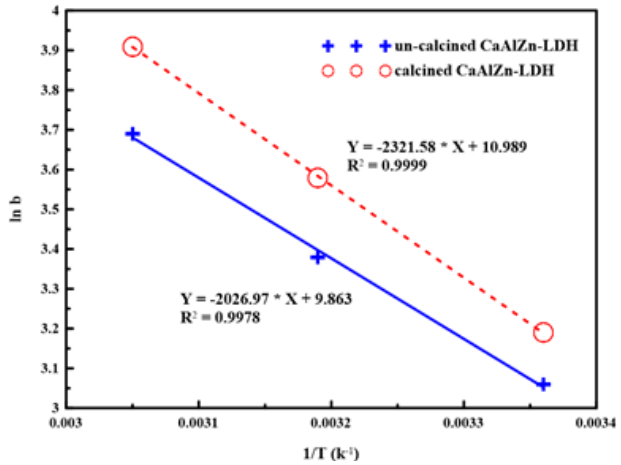

Fig. 7. Plot of the Langmuir isotherm constant (ln b) vs. temperature (1/T) (The thermodynamic parameters in Table 3 are determined from this graph).

of contact time, 115mg/l of initial concentration, 0.25g/l of adsorbent mass, constant pH 6.0 and stirring rate of 160rpm. From the correlation coefficients of Cu(II) adsorption process, the pseudo-first order model at low temperatures (298 and 313k) was more suitable to describe the system and at higher temperatures (328K); the system is more appropriately described by pseudo-second-order model. The homogeneity of active sites on the LDHs surfaces means that the chemisorption reaction is the principal mechanism in the adsorption process and the adsorption process followed Langmuir adsorption model. The thermodynamics parameters indicated a spontaneous cupreous ions removal by adsorbents and the adsorption become more favorable at a higher temperature and there is an endothermic behavior of the adsorption reaction.

Compliance with the ethical statement

All authors of this paper have no conflict of interest with one or organization.

References

1. Foong, C.Y., Wirzal, M.D.H., Bustam, M.A. A review on nanofibers membrane with amino-based ionic liquid for heavy metal removal. Journal of Molecular Liquids., 297, 111793 (2020).
2. Abukhadra, M.R., Sayed, M.A., Rabie, A.M., Ahmed, S.A. Surface decoration of diatomite by Ni/NiO nanoparticles as hybrid composite of enhanced adsorption properties for malachite green dye and hexavalent chromium. Colloids and Surfaces A: Physicochemical and Engineering Aspects., 577, 583-93 (2019).
3. Al-Sherbini, A-S.A., Ghannam, H.E.A., El-Ghanam, G.M.A., El-Ella, A.A., Youssef, A.M. Utilization of chitosan/Ag bionanocomposites as eco-friendly photocatalytic reactor for Bactericidal effect and heavy metals removal. Heliyon., 5(6), e01980 (2019).
4. Rabie, A.M., Abd El-Salam, H.M., Betiha, M.A., El-Maghrabi, H.H., Aman D. Mercury removal from aqueous solution via functionalized mesoporous silica nanoparticles with the amine compound. Egyptian Journal of Petroleum., 28(3), 289-96 (2019).
5. Jawed, A, Saxena, V, Pandey, LM. Engineered nanomaterials and their surface functionalization for the removal of heavy metals: A review. Journal of Water Process Engineering., 33, 101009 (2020).
6. Babel, S., Kurniawan, T.A., Cr(VI) removal from synthetic wastewater using coconut shell charcoal and commercial activated carbon modified with oxidizing agents and/or chitosan, Chemosphere, 54(7), 951–967 (2004).
7. Eccles, H., Treatment of metal-contaminated wastes: why select a biological process?, Trends. Biotechnol., 17, 462–465 (1999).
8. Leung, W.C., Wong, M.F., Chua, H., Lo, W., Leung, C.K., Removal and recovery of heavy metals by bacteria isolated from activated sludge treating industrial effluents and municipal wastewater, Water Sci. Technol., 41(12), 233–240 (2000).
9. Kurniawan, T.A., Chan, G.Y.S., Lo, W.H., Babel, S., Comparisons of low-cost adsorbents for treating wastewaters laden with heavy metals, Sci. Total Environ., 366(2–3), 409–426 (2005).
10. Manirethan, V., Raval, K., Rajan, R., Thaira, H., Balakrishnan, R. M., Kinetic and thermodynamic studies on the adsorption of heavy metals from aqueous solution by melanin nanopigment obtained from marine source: *Pseudomonas stutzeri,* J. Environ. Manage., 214, 315-324 (2018).
11. Hang, Y., Si, Y., Zhou, Q., Yin, H., Wang, A., Cao, A., Morphology-controlled synthesis of calcium titanate particles and adsorption kinetics, isotherms, and thermodynamics of Cd(II), Pb(II), and Cu(II) cations, J. Hazard. Mater., 380, 120789-120802 (2019).
12. Wang, A., Si, Y., Yin, H., Chen, J., Huo, J., Synthesis of Na-, Fe-, and Mg-containing titanate nanocomposites starting from ilmenite and NaOH and adsorption kinetics, isotherms, and thermodynamics of Cu(II), Cd(II), and Pb(II) cations, Mater. Sci. Eng. B, 249, 114411-114419 (2019).
13. Mobasherpour, I., Salahi, E., Ebrahimi, M., Thermodynamics and kinetics of adsorption of Cu(II) from aqueous solutions onto multi-walled carbon nanotubes, J. Saudi Chem. Soc., 18, 792–801 (2014).
14. Gadiri, A., Benkhaled, A., Choukchou-Braham, E., Equilibrium, kinetic and thermodynamic studies of copper adsorption onto poly(n-vinylpyrrolidone) modified clay, J. Macromol. Sci. A, 55(5), 393–400 (2018).
15. Mustapha, S., Shuaib, D. T., Ndamitso, M. M., Etsuyankpa, M. B., Sumaila, A., Mohammed,

U. M., Nasirudeen, M. B., Adsorption isotherm, kinetic and thermodynamic studies for the removal of Pb(II), Cd(II), Zn(II) and Cu(II) ions from aqueous solutions using *Albizia lebbeck* pods, Appl. Water Sci., 9, 142-152 (2019).

16. Bakr, A.A., Eshaq, Gh., Rabie, A.M., Mady, A.H., ElMetwally, A.E., Cupper ions removal from aqueous solutions by novel Ca-Al-Zn layered double hydroxides, Desalin. Water Treat., 57(27), 12632-12643 (2016).

17. Legrouri, A., Lakraimi, M., Barroug, A., Roy, A. D., Besse, J. P., Removal of the herbicide 2,4-dichlorophenoxyacetate from water to zinc-aluminum-chloride layered double hydroxides, Water Res., 39, 3441-3448 (2005).

18. Bakr, A. A., Moustafa, Y. M., Khalil, M. M. H., Yehia, M. M., Motawea, E. A., Magnetic nanocomposite beads: synthesis and uptake of Cu(II) ions from aqueous solutions, Can. J. Chem., 93, 289-296 (2015).

19. Roy, A., Bhattacharya, J., Removal of Cu(II), Zn(II) and Pb(II) from water using microwave-assisted synthesized maghemite nanotubes, Chem. Eng. J. 211-212, 493-500 (2012).

20. Bakr, A. A., Moustafa, Y. M., Khalil, M. M. H., Yehia, M. M., Motawea, E. A., Removal of ferrous ions from their aqueous solutions onto $NiFe_2O_4$-alginate composite beads, J. Environ. Chem. Eng., 3, 1486-1496 (2015).

21. Khalil, M.M.H., Al-Wakeel, K.Z., Abd El Rehim, S.S., Abd El Monem, H., Efficient removal of ferric ions from aqueous medium by amine modified chitosan Resins, J. Environ. Chem. Eng., 1, 566-573 (2013).

22. Bakr, A.A., Mostafa, M.S., Eshaq, Gh., Kamel, M. M., Kinetics of uptake of Fe(II) from aqueous solutions by Co/Mo layered double hydroxide (Part 2), Desalin. Water Treat. 56, 248-255 (2015).

23. Mostafa, M.S., Bakr, A.A., Adsorption of Cd(II) from aqueous solutions via meso structured adsorbent based on Ni/Mo-LDH: kinetics, thermodynamics, and adsorption mechanism, Energ. Source. Part A, 41(18), 2257–2265 (2019).

24. Yakout, S. M., Elsherif, E., Batch kinetics, isotherm and thermodynamic studies of adsorption of strontium from aqueous solutions onto low cost rice-straw based carbons, Carbon – Sci. Tech., 1, 144-153 (2010).

25. Liu, Y., Liu, Y.J., Biosorption isotherms, kinetics and thermodynamics, Sep. Purif. Technol., 61, 229-242 (2008).

26. Mostafa, M.S., Bakr, A.A., Adsorptive removal of Cd(II) from contaminated water via hexavalent molybdenum-containing layered double hydroxide: Ni/Mo-LDH, Energ. Source. Part A, 41(18), 2257–2265 (2019).

27. Bakr, A.A., Sayed, N.A., Salama, T.M., Ali, I. O., Abdel Gayed, R.R., Negm, N.A., Kinetics and thermodynamics of Mn(II) removal from aqueous solutions onto Mg-Zn-Al LDH/montmorillonite nanocomposite, Egypt. J. Pet., 27, 1215–1220 (2018).

28. Emmanuel, K.A., Rao, A.V., Comparative study on adsorption of Mn(II) from aqueous solutions on various activated carbons, E-J. Chem., 6, 693-704 (2009).

29. Bakr, A.A., Makled, W.A., New pretreatment media filtration for SWRO membranes of desalination plants, Desalin. Water Treat., 55(3), 718-730 (2015).

30. Hadi, P., To, M.H., Hui, C.W., Lin, C.S.K., McKay, G., Aqueous mercury adsorption by activated carbons, Water Res. 73, 37-55 (2015).

31. Saini, A.S., Melo, J.S., Biosorption of uranium by melanin: kinetic, equilibrium and thermodynamic studies, Bioresour. Technol., 149, 155-162 (2013).

32. Akpomie, K.G., Dawodu, F.A., Adebowale, K.O., Mechanism on the sorption of heavy metals from binary-solution by a low cost montmorillonite and its desorption potential, Alex. Eng. J., 54, 757-767 (2015).

33. Ali, R.M., Hamad, H.A., Hussein, M.M., Malash, G.F., Potential of using green adsorbent of heavy metal removal from aqueous solutions: adsorption kinetics, isotherm, thermodynamic, mechanism and economic analysis, Ecol. Eng., 91, 317–332 (2016).

34. Badawi, M., Negm, N.A., Abou Kana, M.T.H., Hefni, H.H., Abdel Moneem, M.M., Adsorption of aluminum and lead from wastewater by chitosan-tannic acid modified biopolymers: isotherms, kinetics, thermodynamics and process mechanism, Int. J. Biol. Macromol., 99, 465–476 (2017).

35. Liu, L., Wan, Y., Xie, Y., Zhai, R., Zhanga, B., Liu, J., The removal of dye from aqueous solution using alginate-halloysite nanotube beads, Chem. Eng. J., 187, 210-216 (2012).

36. Shim, J., Lim, J., Shea, P.J., Oh, B.T., Simultaneous removal of phenol, Cu and Cd from water with corn cobsilica-alginate beads, J. Hazard. Mater., 272, 129-136 (2014).

37. Chen, J.H., Liu, Q.L., Hu, S.R., Ni, J.C., He, Y.S., Adsorption mechanism of Cu(II) ions from aqueous solution by glutaraldehyde crosslinked humic acid-immobilized sodium alginate porous membrane adsorbent, Chem. Eng. J., 173(2), 511-519 (2011).

38. Ai, L., Li, M., Li, L., Adsorption of methylene blue from aqueous solution with activated carbon/cobalt ferrite/alginate composite beads: kinetics, isotherms, and thermodynamics, J. Chem. Eng. Data, 56, 3475-3483 (2011).